COMPUTATIONAL MODELLING OF OXIDES' SURFACE TENSIONS IN SECONDARY METALLURGY AND CONTINUOUS CASTING

Eetu-Pekka Heikkinen, Jaana Riipi & Timo Fabritius
University of Oulu, Finland

Risto Pajarre & Pertti Koukkari
VTT Technical Research Centre of Finland

ABSTRACT

Surface tensions of molten multicomponent ionic systems can be modelled based on various assumptions. Two computational models were used to estimate the surface tensions of oxide systems containing SiO_2*, CaO,* Na_2O *and* Al_2O_3 *as a function of temperature and composition. The compositions of the oxide melts were chosen to correspond those of ladle slags in secondary metallurgy and casting powders in the continuous casting of steel.*

The first of two models uses Butler's equation to calculate the surface tensions of the multicomponent melts and is based on the Tanaka et al. [1] consideration of the ionic radii of the components as well as surface tensions and molar volumes of pure components. In the second model the same ionic radii dependent contribution is applied as activity coefficients to a constrained free energy model [2] where the surface layer is considered as a separate phase in the system. In the model, the constrained interfacial area is analogous with a component mass balance in a traditional computation of a multiphase chemical equilibrium and surface energy with the corresponding chemical potential.

The results of the models were compared with experimental values reported in the literature. Based on the results it was concluded that the effect of temperature on the surface tensions of the considered oxide melts was insignificant when compared to the effect of chemical composition. According to the validation the results agreed well with the published surface tension data. The multi-component surface tension approach provides a practical method for evaluation of e.g. functioning of various casting powders in practical steel solidification.

INTRODUCTION

The significance of interfacial phenomena and properties is essential in iron and steelmaking processes since most of the chemical reactions in these processes are heterogeneous and thus involve separate phases that are divided by phase boundaries through which the elements must tranfer. One of the most important boundaries to be considered in the metallurgy of steelmaking is the interface between molten steel and slag due to its influence on the kinetics of various phenomena taking place between the two phases (e.g. sulphur removal, inclusion transfer) [3].

In order to succeed in the production of clean steel with high quality standards, it is necessary to have an accurate control over the slags' compositions and properties. Although the interfacial tension plays an essential role while considering the phenomena on the steel-slag-interface, it is equally important to be familiar with the surface properties of individual phases (i.e. surface tension) in order to understand the behaviour of different phases in the considered systems [3, 4, 5].

Surface tensions of molten multicomponent ionic systems can be modelled using various assumptions. The purpose of this study was to evaluate the applicability of two surface tension models [1, 2] for the prediction of the ladle slag and casting powder properties. The models were used to calculate the surface tensions for the molten multicomponent oxide systems of various compositions after which the computational values were compared with the experimental values that were achieved from the literature [6].

METHODOLOGY

Two computational models were used to estimate the surface tensions of oxide systems containing MnO, MgO, SiO_2, CaO, Al_2O_3, Na_2O and CaF_2. The compositions of the oxide melts that were chosen to correspond those of ladle slags in secondary metallurgy [7] and casting powders in the continuous casting of steel [8] are presented in Table 1.

Table 1: The compositions of oxide melts (in weight-%) that were considered in the calculations

	Al_2O_3	CaO	MgO	SiO_2	MnO	Na_2O	CaF_2	T [°C]
LS-A-1	35.0	50.0	5.0	5.0	5.0	-	-	1600
LS-A-2	36.5	50.5	5.5	5.0	2.5	-	-	1600
LS-A-3	38.0	51.0	6.0	5.0	0.0	-	-	1600
LS-A-4	39.5	51.0	6.0	3.5	0.0	-	-	1600
LS-A-5	41.0	51.0	6.0	2.0	0.0	-	-	1600
LS-B-1	33.0	48.0	5.0	10.0	4.0	-	-	1600
LS-B-2	35.0	48.0	5.0	10.0	2.0	-	-	1600
LS-B-3	37.0	48.0	5.0	10.0	0.0	-	-	1600
LS-B-4	38.5	48.0	5.0	8.5	0.0	-	-	1600
LS-B-5	40.0	48.0	5.0	7.0	0.0	-	-	1600
CP-A-1	5.0	36.0	1.0	43.0	6.0	3.0	6.0	1400
CP-A-2	10.0	33.0	1.0	41.0	6.0	3.0	6.0	1400
CP-B-1	5.0	33.0	1.0	40.0	6.0	9.0	6.0	1400
CP-B-2	10.0	30.0	1.0	38.0	6.0	9.0	6.0	1400
CP-C-1	5.0	33.0	1.0	40.0	6.0	3.0	12.0	1400
CP-C-2	10.0	30.0	1.0	38.0	6.0	3.0	12.0	1400

CP-D-1	5.0	30.0	1.0	37.0	6.0	9.0	12.0	1400
CP-D-2	10.0	27.0	1.0	35.0	6.0	9.0	12.0	1400

LS-A = Ladle Slag with a low initial SiO_2-content. / LS-B = Ladle Slag with a high initial SiO_2-content. / CP-A = Casting powder with low Na_2O and low CaF_2 content. / CP-B = Casting powder with high Na_2O and low CaF_2 content. / CP-C = Casting powder with low Na_2O and high CaF_2 content. / CP-D = Casting powder with high Na_2O and high CaF_2 content.

The compositions presented in Table 1 are based on two different ladle slags (with higher and lower initial SiO_2 content) and four casting powders (with varying Na_2O and CaF_2 contents). In addition to these initial (or fundamental) compositions, the effect of aluminium addition on the surface tensions of both ladle slags and casting powders was considered. The aluminium addition to the ladle slag represents the reduction of the slag which is executed in order to decrease the amount of MnO (cf. LS-A-1 to LS-A-3 and LS-B-1 to LS-B-3 in Table 1) and FeO, latter of which was not considered in this context. Excessive additions of aluminium causes also the reduction of SiO_2 (cf. LS-A-3 to LS-A-5 and LS-B-3 to LS-B-5 in Table 1). The effects of aluminium additions on the slag compositions were estimated with thermodynamic calculations and are reported more accurately by Leinonen *et al.* [7]. Two Al_2O_3 contents (5 w-% and 10 w-%) were used for all four casting powders in order to estimate effect of dissolution of alumina inclusions on the surface tensions of casting powders.

The effect of temperature was also considered, but since it was noticed that its effect on the surface tension was neglible in comparison with the composition changes (at least in the range of interest within this study), it was not used as a variable in the calculations that are presented in this paper.

Tanaka's Model

Tanaka *et al.* have derived a model for the determination of the oxidic melts' surface tensions based on Butler's model which can be used to calculate the surface tensions of the liquid (metal) alloys by solving the unknown parameters (i.e. the surface tension of liquid alloy σ as well as the surface compositions N_i^{Surf} of the components i) from Equations 1 and 2. The Equations 1 and 2 are presented for a binary system A-B. For the multicomponent systems the number of equations is equal to the number of components. The number of unknown variables is one more than the number of components (i.e., the surface tension and the surface compositions of all the components), but since one of the contents can be presented as a function of others (i.e., 100% - the contents of all the other components), the number of real unknowns is equal to that of equations [1].

$$\sigma = \sigma_A^{Pure} + \frac{RT}{A_A} \ln \frac{N_A^{Surf}}{N_A^{Bulk}} + \frac{1}{A_A} \left[G_A^{E,Surf}\left(T, N_B^{Surf}\right) - G_A^{E,Bulk}\left(T, N_B^{Bulk}\right) \right] \quad (1)$$

$$\sigma = \sigma_B^{Pure} + \frac{RT}{A_B} \ln \frac{N_B^{Surf}}{N_B^{Bulk}} + \frac{1}{A_B} \left[G_B^{E,Surf}\left(T, N_B^{Surf}\right) - G_B^{E,Bulk}\left(T, N_B^{Bulk}\right) \right] \quad (2)$$

The symbols presented in Equations 1 and 2 are as follows: subscripts Bulk and Surf represent bulk and surface, respectively; σ_i^{Pure} represents the surface tension of pure component i; $A_i = LN_0^{1/3} V_i^{2/3}$ in which N_0 is Avogadro's number, L equals 1.091 for molten metals and V_i represents the molar volume of pure component i; T is absolute temperature; R is gas constant; N_i^P is a mole fraction of component i in either bulk (P = Bulk) or surface (P = Surf) and $G_i^{E,P}(T, N_B^P)$ is a partial excess Gibbs free energy of component i in either bulk (P = Bulk) or surface (P = Surf) as a function of temperature and the mole fraction of component B. The excess Gibbs free energies for the bulk, $G_i^{E,Bulk}(T, N_B^{Bulk})$, can be obtained directly from thermodynamic databases, whereas the excess Gibbs free energies for the surface, $G_i^{E,Surf}(T, N_B^{Surf})$, are estimated from the approximation proposed by Speiser *et al.* and presented in Equation 3 [1, 9, 10].

$$G_i^{E,Surf}\left(T, N_B^{Surf}\right) = \beta^{MIX} \cdot G_i^{E,Bulk}\left(T, N_B^{Surf}\right) \tag{3}$$

The values of β^{MIX}, which is related to the ratio of the coordination number in the surface to that in the bulk (Z^{Surf}/Z^{Bulk}), cannot be evaluated exactly for the liquid phases, but Tanaka *et al.* [1] have determined it to be 0.83 for pure metals and alloys [1, 9, 10].

Based on the Butler's equation, Tanaka *et al.* [1] have derived a model that takes the surface relaxation of the molten ionic mixtures (such as spontaneous change in ionic distance at the surface) as well as the ratio between the radii of cation and anion into account and is therefore suitable for molten ionic mixtures. The surface structural relaxation is considered in σ_i^{Pure} -terms. Additionally, it causes the excess Gibbs free energies of the surface to approach the excess Gibbs free energies of the bulk. Therefore the difference between the excess Gibbs free energies of the surface and the bulk is neglected. The radii of the ions are taken into account by replacing the mole fractions in Equations 1 and 2 by ionic radius fractions [1].

The equations for the calculation of the surface tension of the binary molten ionic mixture AX-BY, in which A and B represent cations and X and Y represent anions, are presented in Equations 4 and 5. In a binary system there are two unknown variables (i.e., the surface tension and the surface composition of a one species; since the surface composition of another species is attached) and two equations and hence the surface tension of a mixture can be calculated. For the multicomponent systems, the number of equations as well as unknown variables is increased in proportion to the number of species as in the use of Butler's equation [1].

$$\sigma = \sigma_{AX}^{Pure} + \frac{RT}{A_{AX}} ln \frac{M_{AX}^{Surf}}{M_{AX}^{Bulk}} \tag{4}$$

$$\sigma = \sigma_{BY}^{Pure} + \frac{RT}{A_{BY}} ln \frac{M_{BY}^{Surf}}{M_{BY}^{Bulk}} \tag{5}$$

Symbols σ_i^{Pure}, T and R have a same meaning in Equations 4 and 5 as in Equations 1 and 2. A_i equals $N_0^{1/3} V_i^{2/3}$ (N_0 is Avogadro's number and V_i represents the molar volume of pure substance i) and the ionic radius fractions M_i^P can be calculated using Equations 6 and 7 [1].

$$M_{AX}^{P} = \frac{(R_A/R_X)\cdot N_{AX}^P}{(R_A/R_X)\cdot N_{AX}^P + (R_B/R_Y)\cdot N_{BY}^P} = \frac{(R_A/R_X)\cdot N_{AX}^P}{\sum_{i=A}^{B}\sum_{j=X}^{Y}\left[(R_i/R_j)\cdot N_{ij}^P\right]} \tag{6}$$

$$M_{BY}^{P} = \frac{(R_B/R_Y)\cdot N_{BY}^P}{(R_A/R_X)\cdot N_{AX}^P + (R_B/R_Y)\cdot N_{BY}^P} = \frac{(R_B/R_Y)\cdot N_{BY}^P}{\sum_{i=A}^{B}\sum_{j=X}^{Y}\left[(R_i/R_j)\cdot N_{ij}^P\right]} \tag{7}$$

in which R_i is a radius of an ion i and N_i^P is a mole fraction of species i in either bulk (P = Bulk) or surface (P = Surf). Subscripts A and B represent cations and X and Y represent anions whereas the superscript P (equals either Bulk or Surf) indicates the bulk and the surface, respectively [1].

The values of surface tensions and molar volumes of the pure liquid oxides as well as radii of the cations and anions used in the calculations were achieved from the literature [11, 12] and are presented in Table 2.

Table 2: Initial values for the calculations

	σ_i^{Pure} [mN·m^{-1}]	V_i[m^3·mol^{-1}]	R_A	R_X
SiO_2	$243.2 + 0.031\cdot T$	$27.516\cdot[1+10^{-4}(T-1773)]\cdot 10^{-6}$	0.42 Å [1]	1.44 Å [1]
Al_2O_3	$1024 - 0.177\cdot T$	$28.3\cdot[1+10^{-4}(T-1773)]\cdot 10^{-6}$	0.51 Å [2]	1.44 Å [2]
CaO	$791 - 0.0935\cdot T$	$20.7\cdot[1+10^{-4}(T-1773)]\cdot 10^{-6}$	0.99 Å	1.44 Å
MgO	$1770 - 0.636\cdot T$	$16.1\cdot[1+10^{-4}(T-1773)]\cdot 10^{-6}$	0.66 Å	1.44 Å
MnO	$988 - 0.179\cdot T$	$15.6\cdot[1+10^{-4}(T-1773)]\cdot 10^{-6}$	0.80 Å	1.44 Å
Na_2O	$438 - 0.116\cdot T$	$33.0\cdot[1+10^{-4}(T-1773)]\cdot 10^{-6}$	0.97 Å	1.44 Å
CaF_2	$1604.6 - 0.72\cdot T$	$31.3\cdot[1+10^{-4}(T-1773)]\cdot 10^{-6}$	0.99 Å	1.33 Å

[1] Since SiO_4^{4-} exists in molten silicate systems, it was assumed that Si^{4+} is a cation and SiO_4^{4-} is an anion while evaluating the ratio of cationic and anionic radii. In the calculations of this study, the value of 0.5 presented by Tanaka *et al.* [1] was used.

[2] Al_2O_3 could be assumed to have a cation of Al^{3+} and an anion of AlO_3^{3-} in the ionic melts. However, the ratio of the radii of these ions was not available and therefore the values presented in this table for R_{Al3+} and R_{O2-} were used in the calculations within this study.

Constrained Free Energy Method

Using constrained free energy (CFE) method, Butler model type behaviour is achieved by defining the surface layer as a new phase [2, 13]. The equilibrium condition of constant surface area is applied by defining a new component whose stoichiometric coefficients are proportional to the molar areas of the corresponding species in the surface layer and zero in the bulk. The total area in the system can be chosen arbitrarily as long as it is non zero, but small enough that the equilibration of the surface phase does not have noticeably effect on the composition of the bulk.

The surface tension is the difference between the Gibbs free energy per unit surface area between the modelled state and a state where all the material would be in the bulk state:

$$\sigma = \frac{\overline{G}_i^{Surf} - \overline{G}_i^{Bulk}}{A_i} = \frac{\pi_{area}}{A_0} \tag{8}$$

where $\overline{G}_i^{Surf}$ and $\overline{G}_i^{Bulk}$ are the molar Gibbs free energies of species *i* in the surface and in the bulk phase (the latter being equal to the chemical potential of the same species), π_{area} is the chemical potential (using the Lagrange method for Gibbs energy minimisation it appears as an additional Lagrangian multiplier) of the new component used to impose the constant surface area condition and A_0 the normalisation constant used to convert the molar surface area of each species to corresponding dimensionless stoichiometric coefficient. Surface tension of each pure substance in the model is set by adjusting correspondingly the standard state chemical potentials:

$$\mu_i^{0,Surf} = \mu_i^{0,Bulk} + A_i \sigma_i \tag{9}$$

where $\mu_i^{0,Surf}$ and $\mu_i^{0,Bulk}$ are the standard state chemical potentials of species *i* in the surface and bulk phases respectively. With these definitions the chemical equilibrium condition in the system becomes the one presented in Equation 10:

$$\mu_i^{0,Bulk} + RT\ln a_i^{Bulk} = \mu_i^{0,Surf} + RT\ln a_i^{Surf} - A_i\sigma \tag{10}$$

Butler relation (Equations 1 and 2) is achieved by solving σ from Equation 10. In using the Tanaka's model for salt mixtures the ratio between cation and anion radii is applied as they were activity coefficients for individual salts, leading to the relationship presented in Equations 4, 5, 6 and 7.

The actual equilibrium composition and properties were solved by multipurpose Chemical equilibrium calculator ChemSheet [14]. The main benefit of using such a program is that the systems can be of near arbitrary complexity (with ChemSheet maximum of 30 components but up to hundreds of species).

The initial values needed for the modelling (i.e. the values of surface tensions and molar volumes of the pure liquid oxides as well as radii of the cations and anions) were equal to ones that were used in Tanaka's model (cf. Table 2).

RESULTS

The computational surface tensions according to both Tanaka's model and constained free energy model for the systems presented in Table 1 are presented in Figure 1.

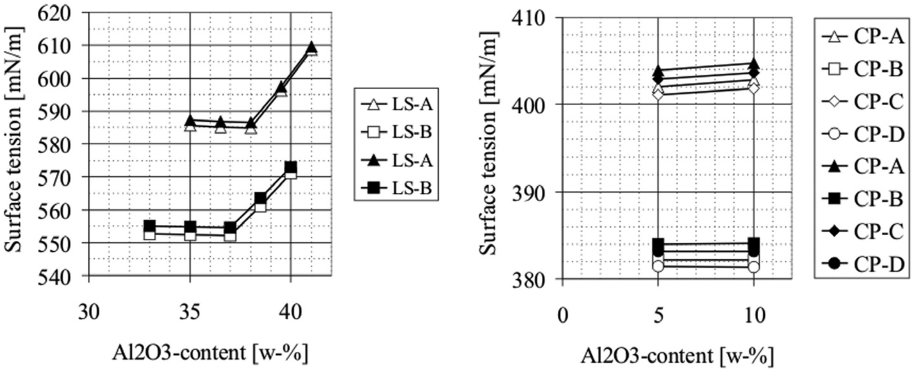

(a) (b)

Figure 1: Surface tensions of the ladle slags (a) and casting powders (b) as a function of Al_2O_3-content according to Tanaka's model (open markers) and CFE method (closed markers)

When considering the results presented in Figure 1(a), one should notice that although the results are presented as function of Al_2O_3 content, it is not the only change that occurs in the composition (cf. Table 1). As the Al_2O_3 content of the ladle slag increases, the content of MnO decreases from 4-5% to zero after which the excessive Al_2O_3 addition leads up to a decrease in the SiO_2 content as well [7]. It is seen from Figure 1 that the surface tension of the slag does not increase until the SiO_2 content begins to change. The increase of Al_2O_3 content in the casting powders (i.e. Figure 1(b)) causes decreases in the contents of CaO and SiO_2, although the CaO/SiO_2 -ratio remains approximately constant.

Experimental data for the exact compositions presented in Table 1 was not available in the literature, since the amount of reported data for the multicomponent systems is rather limited in general. However, experimental values for four ternary systems (Al_2O_3-CaO-MgO; Al_2O_3-CaO-SiO_2; CaO-SiO_2-CaF_2; CaO-SiO_2-Na_2O) and one five-component system (Al_2O_3-CaO-SiO_2-Na_2O-CaF_2) that were close to the compositions used in this study were obtained from the literature [6]. These values were compared with the computational values that were calculated for the similar compositions by using both Tanaka's model and constrained free energy model. The comparison of computational and experimental values is presented in Table 3 and Figure 2.

Table 3: Comparison of computational and experimental values

Al_2O_3 [w-%]	CaO [w-%]	MgO [w-%]	SiO_2 [w-%]	Na_2O [w-%]	CaF_2 [w-%]	T [°C]	σ[$mN \cdot m^{-1}$] Tanaka	σ[$mN \cdot m^{-1}$] CFE	σ[$mN \cdot m^{-1}$] [6]
41	49	10	-	-	-	1600	625	625	580
43	52	5	-	-	-	1600	628	628	570
44	55	-	1	-	-	1600	621	621	653
35	53	-	12	-	-	1600	543	546	573
42	52	-	6	-	-	1600	580	582	624
-	47	-	47	-	6	1600	405	407	434
-	41	-	44	-	15	1600	380	382	381
-	34	-	51	-	15	1600	364	366	337
-	44	-	53	3	-	1590	396	398	366
-	39	-	48	13	-	1590	362	364	327
10	40	-	40	5	5	1400	400	402	432
10	40	-	30	5	15	1400	413	415	386
10	35	-	45	5	5	1400	387	387	420
10	25	-	45	5	15	1400	373	374	380

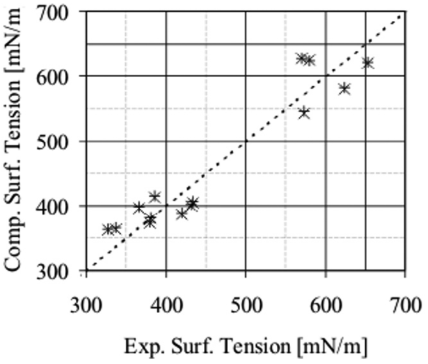

Figure 2: Comparison of computational and experimental values (x = Tanaka's model; + = CFE method)

DISCUSSION

It is seen from Figure 1(a) and Table 3 that the Al addition to the ladle slags has a neglible effect on the surface tension as long as the increase of Al_2O_3-content is related to a decrease of MnO-content (i.e., Al_2O_3-contents from 35 to 38 w-% for LS-A and from 33 to 37 w-% for LS-B in Figure 1). Excessive Al addition causes SiO_2 to be reduced in addition to MnO [7] which in turn leads up to a decrease in the SiO_2-content as the Al_2O_3-content increases (cf. from LS-A-3 to LS-A-5 as well as from LS-B-3 to LS-B-5 in Table 1). This has an increasing influence on the slag's surface tension and could be observed with both ladle slag compositions (i.e., LS-A and LS-B in Table 1 and Figure 1(a)). In addition to its influence on the slag's surface and interfacial properties, the excessive Al addition could cause problems in the production of certain steel grades also due to increased Si-contents in steel which are caused by the reduction of SiO_2 by the added aluminium [7].

The changes in the surface tensions of the casting powders were insignificant when the Al_2O_3-content was increased from 5 to 10 w-% or when the CaF_2-content was increased from 6 to 12 w-% (i.e., from CP-A to CP-C or from CP-B to CP-D in Table 1 and Figure 1(b)). On the other hand, the increase in the Na_2O-content from 3 to 9 w-% had a decreasing effect on the surface tension (i.e., from CP-A to CP-B or from CP-C to CP-D in Table 1 and Figure 1(b)). Although direct quantitative comparisons between surface and interfacial tensions cannot be made, it could be noted qualitatively that according to Cramb *et al.* [15] the interfacial tension between a stainless steel melt and molten CaO-SiO_2-CaF_2-Na_2O/Al_2O_3 -slag (with a composition close to the ones used in this study with an exception of higher CaF_2-content) increases with increasing Al_2O_3-content (up to w-20%) and decreases with increasing Na_2O-content (up to 15 w-%). The trend concerning the influence of Na_2O seems to be similar to surface tension in this study and to interfacial tension defined by Cramb *et al.* [15], whereas there is a difference in the effect of Al_2O_3. While considering the interfacial properties one should also be aware that according to Mills *et al.* [16] the interfacial tension between a metal and a slag is mainly influenced by the surface tension of metal, not slag.

The comparison of experimental and computational values showed that the results were basically in a rather good accordance with each other (the average difference between experimental and computational values being 6.6%). The comparison of the computational results obtained from two models revealed that the deviations in the results were almost neglible (1.9 mN/m or 0.3% for the systems in which the surface tensions of the ladle slags were considered and 1.9 mN/m or 0.5% for the systems in which the surface tensions of the casting powders were considered).

CONCLUSIONS

Two computational models were used the estimate the surface tensions of molten multicomponent ionic systems with the compositions corresponding those of ladle slags in secondary metallurgy and casting powders in the continuous casting of steel. The computational values were compared with each other and with the experimental values obtained from the literature.

From the results it could be concluded, that the surface tensions of the multicomponent systems (up to seven components) could be modelled computationally with an average error of 6.6%. The results also indicated that the deviation between computational values obtained from the two models were almost neglible. This implies that the modelling of the surface tensions of the multicomponent oxide systems can be executed by considering the surface area as an additional constraint in the total Gibbs free energy of the system.

ACKNOWLEDGEMENTS

This research was financially supported by Finnish Funding Agency for Technology and Innovation (Tekes) as well as Outokumpu Stainless and Ruukki, which are kindly acknowledged by the authors. The authors would also like to thank Paavo Hooli and Topi Ikäheimonen from Outokumpu Stainless for many fruitful discussions concerning the topic.

REFERENCES

Tanaka, T., Kitamura, T. & Back, A. (2006). *Evaluation of Surface Tension of Molten Ionic Mixtures.* ISIJ International, Vol. 46, No. 3, pp. 400-406. [1]

Pajarre, R., Koukkari, P., Tanaka, T. & Lee, J. (2006). *Computing Surface Tensions of Binary and Ternary Systems with the Gibbs'ian Method.* Calphad, Vol. 30, No. 2, pp. 196-200. [2]

Olette, M. (1993). *Surface Phenomena: a Cornerstone of Iron and Steelmaking Processes.* ISIJ International. Vol. 33, No. 10, pp. 1113-1124. [3]

Strandh, J., Nakajima, K., Eriksson, R. & Jönsson, P. (2005). *Solid Inclusion Transfer at a Steel-Slag Interface with Focus on Tundish Conditions.* ISIJ International. Vol. 45, No. 11, pp. 1597-1606. [4]

Strandh, J., Nakajima, K., Eriksson, R. & Jönsson, P. (2005). *A Mathematical Model to Study Liquid Inclusion Behavior at the Steel-Slag Interface.* ISIJ International, Vol. 45, No. 12, pp. 1838-1847. [5]

Verein Deutscher Eisenhüttenleute (1995). Slag Atlas. 2nd edition. Verlag Stahleisen GmbH. Düsseldorf, Germany, p. 616. [6]

Leinonen, M., Heikkinen, E. P., Ollila, S. & Lilja, J. (2008). *Improvement of the Ladle Slag Reduction Practice based on Industrial Trials and Thermodynamic Calculations.* Scanmet III - 3rd International Conference on Process Development in Iron and Steelmaking. 8-11.6.2008. Luleå, Sweden. MEFOS, Vol. 2, pp. 305-314. [7]

Heikkinen, E. P. & Vatanen, J. (2005). *Computational Study on the Solubility of Al_2O_3 and its E Effect on the Viscosities of Casting Powders.* University of Oulu, Department of Process and Environmental Engineering Report, p. 17 [In Finnish]. [8]

Speiser, R., Poirier, D. R. & Yeum, K. (1987). *Surface Tension of Binary Liquid Alloys.* Scripta Metallurgica, Vol. 21, No. 5, pp. 687-692. [9]

Yeum, K., Speiser, R. & Poirier, D. R. (1989). *Estimation of the Surface Tensions of Binary Liquid Alloys.* Metallurgical Transactions B., Vol. 20B, pp. 693-703. [10]

Nakamoto, M., Kiyose, A., Tanaka, T., Holappa, L. & Hämäläinen, M. (2007). *Evaluation of the Surface Tension of Ternary Silicate Melts Containing Al_2O_3, CaO, FeO, MgO or MnO.* ISIJ International, Vol. 47, No. 1, pp. 38-43. [11]

Nakamoto, M., Tanaka, T., Holappa, L. & Hämäläinen, M. (2007). *Surface Tension Evaluation of Molten Silicates Containing Surface-active Components (B_2O_3, CaF_2 or Na_2O).* ISIJ International, Vol. 47, No. 2, pp. 211-216. [12]

Koukkari, P. & Pajarre, R. (2006). *Calculation of Constrained Equilibria by Gibbs Energy Minimization.* Calphad, Vol. 30, No. 2, pp. 18-26. [13]

http://www.chemsheet.com/ [Online].[14]

Cramb, A. W., Chung, Y., Harman, J., Sharan, A. & Jimbo, I. (1997). *The Slag-Metal Interface and Associated Phenomena.* V International Conference on Molten Slags, Fluxes and Salts. 5-8.1.1997. Sydney, Australia. Iron & Steel Society, pp. 35-50. [15]

Mills, K. C., Fox, A. B., Thackray, R. P. & Li, Z. (2004). *The Performance and Properties of Mould Fluxes.* VII International Conference on Molten Slags, Fluxes and Salts. 25-28.1.2004. Cape Town, South Africa. The South African Institute of Mining and Metallurgy, pp. 713-721. [16]